Supplemental Information

A stable high-voltage lithium-ion battery realized by an in-built water scavenger

Zhi Chang,[2,3†] Yu Qiao,[2†] Han Deng,[1,2,3] Huijun Yang,[2,3] Ping He[1] and Haoshen Zhou[1,2,3*]

Affiliations:

[1]Center of Energy Storage Materials & Technology, College of Engineering and Applied Sciences, Jiangsu Key Laboratory of Artificial Functional Materials, National Laboratory of Solid State Micro-structures, and Collaborative Innovation Center of Advanced Micro-structures, Nanjing University, Nanjing 210093, P. R. China.

[2]Energy Technology Research Institute, National Institute of Advanced Industrial Science and Technology (AIST), 1-1-1, Umezono, Tsukuba 305-8568, Japan.

[3]Graduate School of System and Information Engineering, University of Tsukuba,

1-1-1, Tennoudai, Tsukuba 305-8573, Japan.

*Correspondence to: hs.zhou@aist.go.jp & hszhou@nju.edu.cn.

EXPERIMENTAL PROCEDURES

Materials and Methods

All the chemicals employed in this synthesis section were purchased from Wako Pure Chemical Industries Ltd. without additional exception.

Preparation of LiNi$_{0.5}$Mn$_{1.5}$O$_4$ (LNMO) spinel cathode

(1) Preparation of MnCO$_3$ microspheres

Manganese sulphate (MnSO$_4$·H$_2$O, 1.014 g) and sodium bicarbonate (NaHCO$_3$, 4.64 g) were thoroughly dissolved in 2400 mL distilled water, respectively. Then, ethanol (40 mL) was added to the MnSO$_4$ solution under vigorous magnetic stirring, followed by the adding of the NaHCO$_3$ solution. The mixed solution was aged for 3 hours at room temperature (25 °C). The obtained MnCO$_3$ was further centrifuged and washed for 3 times using water and alcohol solution, and then dried at 80 °C for 2 hours in vacuum.

(2) Synthesis of yolk-structured MnO$_2$ microspheres

The obtained MnCO$_3$ (0.4 g, insoluble) microsphere was uniformly dispersed into 80 mL water and stirred for 1 hour. Then 40 mL KMnO$_4$ solution (0.032 mol/L) was slowly added and vigorously stirred for 1 hour. The core-shell MnCO$_3$@MnO$_2$ microspheres were obtained when the solution transformed from purple to dark brown. Then 80 mL of 1.2 mol/L HCl was added and the mixture solution was then stirred for 4 min followed by a rapid centrifuging step. After HCl etching, the yolk structured MnCO$_3$(core)@MnO$_2$(shell) micro-spheres were prepared. The as-obtained powder was washed (with water and alcohol solution) for six times and dried at 80 °C for 1 hour in vacuum. Finally, the as-prepared yolk-structured MnCO$_3$(core)@MnO$_2$(shell) microsphere was further oxidized to pure yolk-structured MnO$_2$ microsphere by additional heat treatment (400 °C for 10 hours).

(3) Synthesis of yolk-structured LiNi$_{0.5}$Mn$_{1.5}$O$_4$ microspheres

The as-prepared yolk-structured MnO$_2$ microsphere was mixed and ground with lithium hydroxide mon-hydrate (LiOH·H$_2$O)$_2$ and Nickel nitrate hexahydrate (Ni(NO$_3$)$_2$·H$_2$O) in the stoichiometric molar ratio (Li: Ni: Mn=1.05: 0.5: 1.5). Then the mixtures were calcined at 800 °C for 20 hours in air atmosphere.[1]

The LiNi$_{0.6}$Co$_{0.2}$Mn$_{0.2}$O$_2$ and LiNi$_{0.8}$Co$_{0.1}$Mn$_{0.1}$O$_2$ (NCM-622 and NCM-811) cathode materials were provided by Prof An-Min Cao in Key Laboratory of Molecular Nanostructure and Nanotechnology, Beijing National Laboratory for Molecular Sciences, Institute of Chemistry, Chinese Academy of Sciences (CAS), Beijing, People's Republic of China. The LiNi$_{0.3}$Co$_{0.3}$Mn$_{0.3}$O$_2$ (NCM-333) was purchased from Amperex Technology Limited Company (ATL), China.

Electrolytes

LiPF$_6$-EC/DMC electrolyte was purchased from Wako Pure Chemical Industries Ltd. The pre-dried electrolyte was prepared by adding CaH$_2$ into the LiPF$_6$-EC/DMC electrolyte (none pre-dried) used in our glove box. Electrolytes with different water contents were prepared by

adding corresponding amount of water into commercial $LiPF_6$-EC/DMC electrolyte (200, 500, 600 and 800 ppm defined as E-200, E-500, E-600 and E-800). The exact water concentrations in electrolytes were measured by Karl Fischer titration.

Preparation of CuBTC MOF film

(1) Preparation of CuBTC powder

CuBTC powder was prepared by firstly dissolved 0.24 g cupric nitrate trihydrate $(Cu(NO_3)_2 \cdot 3H_2O)$ in 25 mL ethanol and 0.105 g 1,3,5-Benzenetricarboxylic Acid (BTC) in 25 ml ethanol, respectively. Then, the two solutions were mixed together followed by stirring for 2 hours.[2] The blue CuBTC powder was washed with ethanol for six times. Then, the prepared CuBTC crystals were immersed in ethanol for 36 hours, and the ethanol solvent was replenished for 3 times before the centrifugation. The CuBTC crystals were firstly dried at 80 °C for 12 hours before final vacuumed at 180 °C for 72 hours to generate the activated CuBTC powder sample.[2]

(2) Fabrication of flexible CuBTC MOF film

Flexible CuBTC MOF film was prepared by thoroughly mixing 90 wt. % activated MOFs samples with 10 wt% polyvinylidene difluoride (PVDF) in dimethylformamide (DMF).[3] The MOFs slurries were then uniformly spread on the Al foil and then dried at 80 °C for 10 min in drying oven. The MOF coated Al foil was then immersed into methanol for 5 min until the MOF film was detached from the Al foil and formed the flexible MOF film. The obtained MOF film was firstly dried at 80 °C for 1 hour in drying oven and then followed by vacuumed dried oven at 180 °C overnight to activate the MOF film. The prepared activated MOF film was then cutted into small plates (16 mm in diameter) and re-activated under vacuum at 180 °C overnight before transferred into glove box for cell assemble. It worth noting that the weight of commercial Celgard and CuBTC MOF separators were tested to be 1.7 and 4.5 mg/cm^2, respectively. Moreover, the corresponding thicknesses of the two separators were 15 and 30 μm, respectively.

Electrodes Preparation

The obtained LNMO, NCM-333, NCM-622, NCM-811 and lithium foil (Lion Chemical Industry Co., Ltd.) were employed as electrode materials. Generally, 0.2 g electrode powders were stirring into a binder gel solution, which composed by polyvinylidene fluoride (PVDF, Du Pont-Mitsui Fluorochemicals Co. Ltd.) powder and N-methyl pyrrolidine (NMP, Sigma Aldrich, 99%) solvent (PVDF:NMP=6:94 wt%). The obtained slurry was then homogeneously coated onto Al foil current collector by a scraper. After tiny pressing procedure, the active materials-loaded metal foil was vacuum dried at 110 °C overnight, and final electrode plates (11 mm in diameter) were punched out. The mass loading of the cathode materials were about 3.0-3.2 mg/cm^2.

Cell Assembly and Electrochemical Measurements

CR2032 coin cells were assembled in an argon-filled glove box, in which both the moisture and oxygen contents were controlled to be less than 1 ppm. The normal (without pre-dried) electrolyte was 1 M $LiPF_6$-EC/DMC with a volume ratio of 1:1. Cathodes, Glass Fiber, MOF

film and lithium anode were orderly placed into 2032 coin-type cells followed by adding electrolytes within different various water contents (50 µL for each cell). The cells were operated with a potential limit between: 3.0-4.9 V (for Li//LNMO cell) and 2.7-4.4 V (Li//NCM-333, Li//NCM-622 and Li//NCM-811 cell) in the study. Before each electrochemical characterization, the cells were kept on open circuit for 10 hours. All of the potentials in this study were referenced to Li/Li$^+$. For 2032 coin-type cells, the galvanostatic electrochemical measurements were carried out under potential control using the battery tester system HJ1001SD8 (Hokuto Denko) at 25 °C. Typically, the characterizations of the cell were carried out under galvanostatic control at the specific current density from the open-circuit potential (OCP) unless other noted. For the EIS and CC-CV mode tests, the electrochemical experiments were carried out under the control of a potentiostat (Potentiostat/Galvanostat PGSTAT30, Autolab Co. Ltd., Netherlands) at room temperature. The current and potential outputs from the potentiostatic were recorded by a multifunction data acquisition module/amplifier (PGSTAT30 Differential Electrometer, Autolab), which was controlled by General Purpose Electrochemical Software (GPES). For the specific test conditions, we will show them in their corresponding sections in related supplementary figures.

Characterizations

SEM, XRD and XPS Characterizations

The morphology of the as-prepared products was characterized with scanning electron microscopy (SEM, JEOL JSM-6380LV FE-SEM). X-ray photoelectron spectroscopy (XPS) was performed using a VG scientific ESCALAB 250 spectrometer with monochromic Al Kα excitation (1486.6 eV). X-ray diffraction (XRD) measurements were performed on a Bruker D8 Advanced diffractometer fitted with Cu-Kα X-rays (λ =1.5406Å) radiation at a scan rate of 0.016 °/s. For the pre-treatment procedures: The cycled cells were transferred into an Ar glove box once the electrochemical treatments were finished, and the electrodes were extracted from the cell and placed in a glass bottle. The electrode plates were twice rinsed by dimethoxyethane (DME, Sigma Aldrich, 99%) to wash off the electrolyte salt and the residual solvent, and then evaporated in a vacuum chamber, connected to the glove box, for 12 hours. The dried electrode plates were moved back to glove box and placed onto a SEM or XPS sample holder. The sample holder was sealed in an airtight container and then transferred into the SEM or XPS sample loading chamber. Note that, in order to restrain the exposure time to the ambient, samples (cycled electrode plates) were tightly sealed into a glass bottle (fill with Ar gas), and transferred to the related chambers (SEM and XPS) as quickly as possible. Thus, we assumed the morphology and the component of electrode surface would not obviously change for such a short time exposure to the open air.

Nuclear Magnetic Resonance (NMR) Spectroscopy Characterizations

The NMR spectra were recorded using a spectrophotometer (500 MHz Ultra-ShieldTM, Bruker). Typically, 256/128 (^{1}H/^{19}F) times were accumulated for one spectrum. The electrodes and separators were extracted from the cycled cells without further pretreatment. 750 µL of D$_2$O (99.9 atom % D, Wako Chemicals) was used to extract the residual electrolyte and soluble parasitic products (mainly carboxylates and fluorides) from the electrodes and the separators, then the solution was transferred to septa-sealed NMR tube. To quantify the amount of related components, 1 µL of benzene (C$_6$H$_6$, Sigma Aldrich, 99%) and 1 µL of fluorobenzene (C$_6$H$_5$F,

Sigma Aldrich, 99%) were mixed and injected through the septa and employed as an internal standard. The method here was very similar as the ones introduced in our previous works.[4,5]

Inductively-Coupled Plasma (ICP) Characterizations

ICP-OES (optical emission spectroscopy) results were recorded using Thermo Scientific iCAP 5600 and PerkinElmer Optima 4300 DV. Metal dissolutions from the LNMO, NCM-622-based electrodes were quantitatively confirmed measuring the Mn and Ni-ion concentrations both in the electrolyte solutions and on the lithium-metal anode.[6] The cycled separators (infiltrated by cycled electrolyte solutions) and lithium electrodes were bathed in DME solvent for 4 hours aging. The separator was salvaged out then the DME solution and Li anode were mixed with a mixture of concentrated hydrochloric acid and nitric acid mixture (3:1 in volume ratio). The solution was heated in a microwave for 2 hours (150 °C).
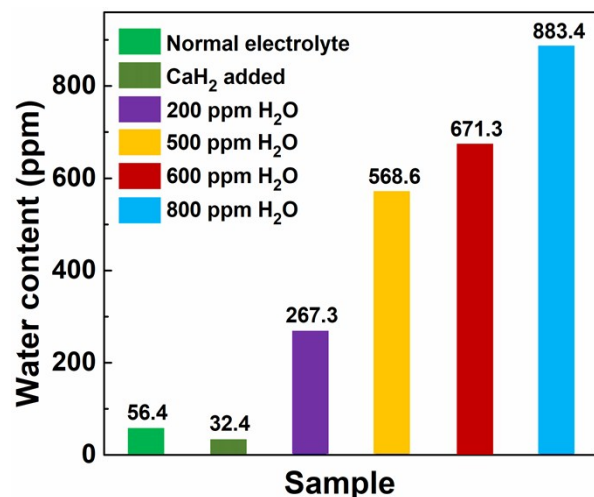
Figure S1. Accurate water contents in various electrolytes with different water additions. The water content for the none pre-dried commercial electrolyte (without pre-dried) used in this work was tested to be 56.4 ppm while the pre-dried electrolyte (using CaH_2 as the chemical drier, 50 mg CaH_2 added in 1 mL commercial electrolyte) maintain a lower value of 32.4 ppm. Certain amount of water (200, 500, 600 and 800 ppm) were deliberately added to the normal electrolytes for further usage and demonstrated the exact water content to be 267.3, 568.6, 671.3 and 883.4 ppm. The prepared various water contained electrolytes were defined as E-200, E-500, E-600 and E-800, respectively.
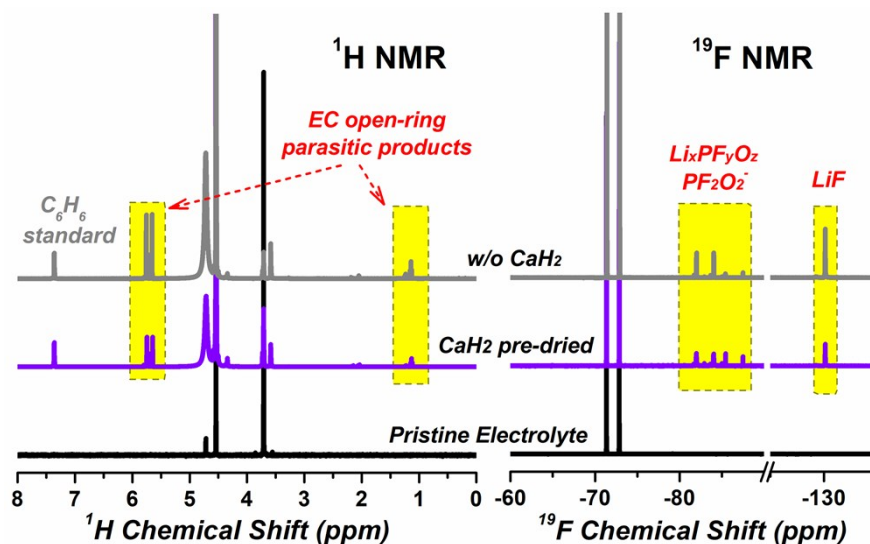
Figure S2. The pre-dried electrolyte enables suppressed detrimental effects induced by water contained in electrolytes for Li//LiNi$_{0.5}$Mn$_{1.5}$O$_4$ (LNMO) batteries. ^{1}H (left) and ^{19}F NMR (right) analysis results of cycled electrolytes from two cells using commercial electrolyte without pre-dried (grey traces) and pre-dried electrolyte (purple traces) after cycling for 100 cycles. ^{1}H and ^{19}F NMR spectra of D$_2$O extracted components from cycled electrolytes. The spectra of the pristine electrolytes are shown on the bottom (black traces). By normalizing the peak of C$_6$H$_6$ inner standard, the degradation products are quantitatively estimated. The EC open-ring parasitic products and the formation of LiF can be clearly observed in LNMO cell using commercial electrolyte without pre-dried, while that of the electrolyte extracted from LNMO cell using pre-dried electrolyte shown alleviated electrolyte decomposition parasitic products and accumulation of HF-related side reaction products.
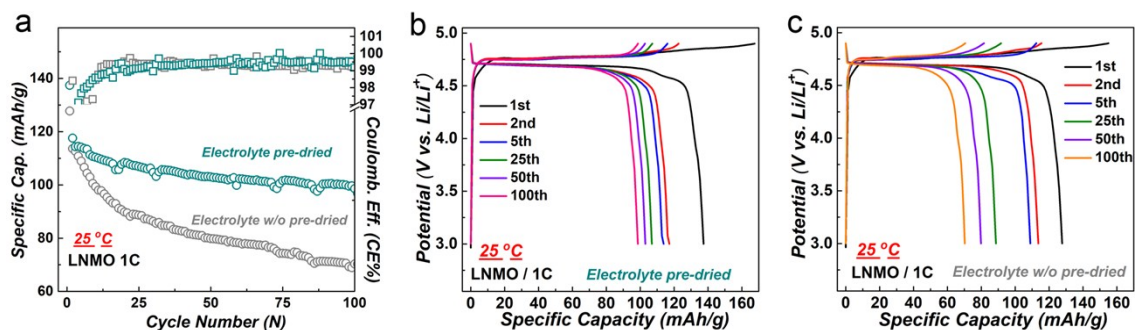
Figure S3. Electrochemical performances of the Celgard separator based Li//LNMO (LNMO) cells. (a) Cycling performances of the LNMO cells cycled in commercial electrolyte without (w/o) pre-dried (grey trace) and pre-dried electrolyte (dark green trace) at 1 C current rate in room temperature of 25 °C and (b and c) the corresponding charge/discharge curves. The LNMO cell using pre-dried electrolyte exhibited enhanced cycling stability compared with the one cycled in un-dried electrolyte.
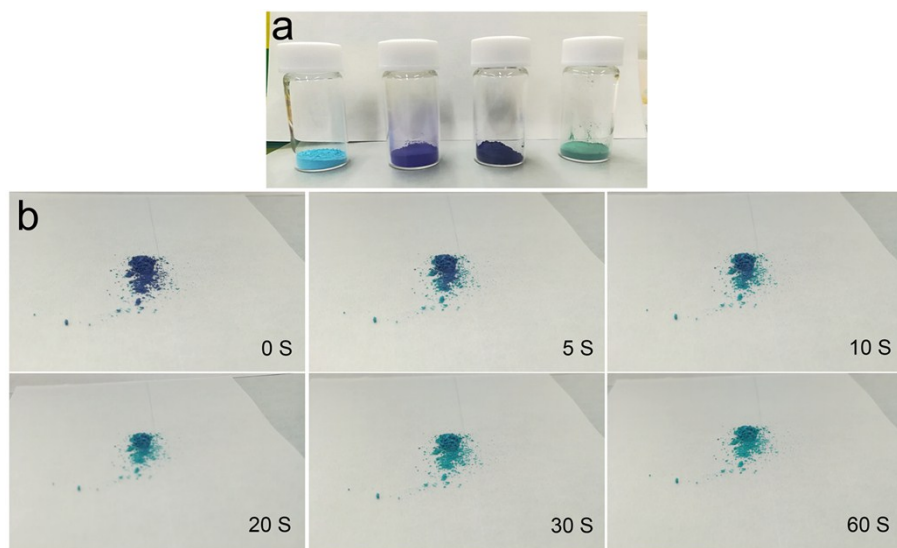
Figure S4. The reversible water adsorbing and desorbing ability of the MOF powders. Color changes of the obtained MOF powders (from left to right) (a) dried at 60 °C for 6 hours in air atmosphere, dried at 180 °C for 24 hours in vacuum, dried at 180 °C for 72 hours in vacuum and the dried/activated MOF powder (180 °C for 72 hours) re-adsorbs water in the air. (b) Quick water absorption of the dried/activated MOF powder (180 °C for 72 hours) within 60 seconds after exposed to air.
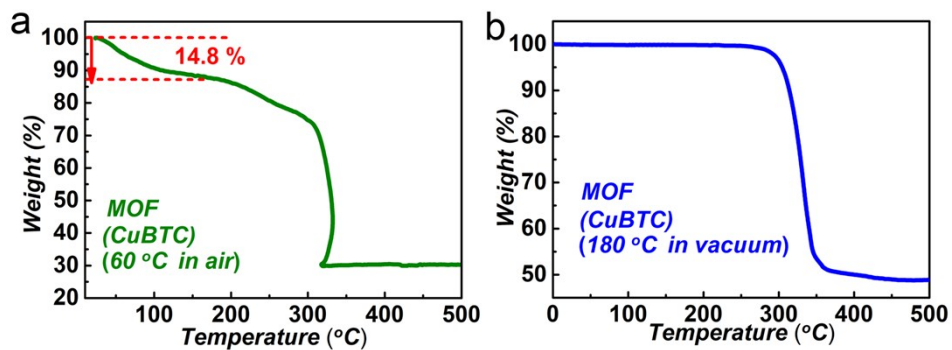
Figure S5. TG curves of the MOF powders. (a) MOF pre-dried in air at 60 °C for 6 hours and (b) MOF dried/activated at 180 °C for 72 hours. TG curve of the CuBTC powder (60 °C dried in air) verifies the co-existence of both the coordinated and the pore-filled water inside CuBTC cavities. All of them can be completely removed by thermal heating at 180 °C under vacuum.
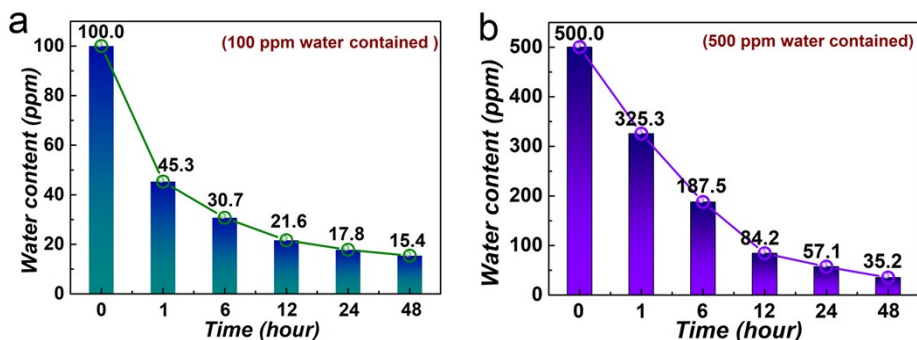
Figure S6. Excellent water adsorption ability of the obtained activated MOF powder. 50 mg MOF powder immersed into 1 mL (a) 100 and (b) 500 ppm water contained electrolytes to test the accurate amount of the remained water after several hours. After 48 hours, water content in 100 ppm water added electrolyte was tested to be 15.4 ppm, which is much lower than that of the CaH_2 pre-dried electrolyte (dropped from original 56.4 ppm to 32.4 ppm). Even tested in a high water content of 500 ppm added electrolyte, the MOF powder can still maintained a good water adsorption performance which was comparable to that of the CaH_2 pre-dried electrolyte (35.2, 32.4 ppm for MOF and CaH_2, respectively).
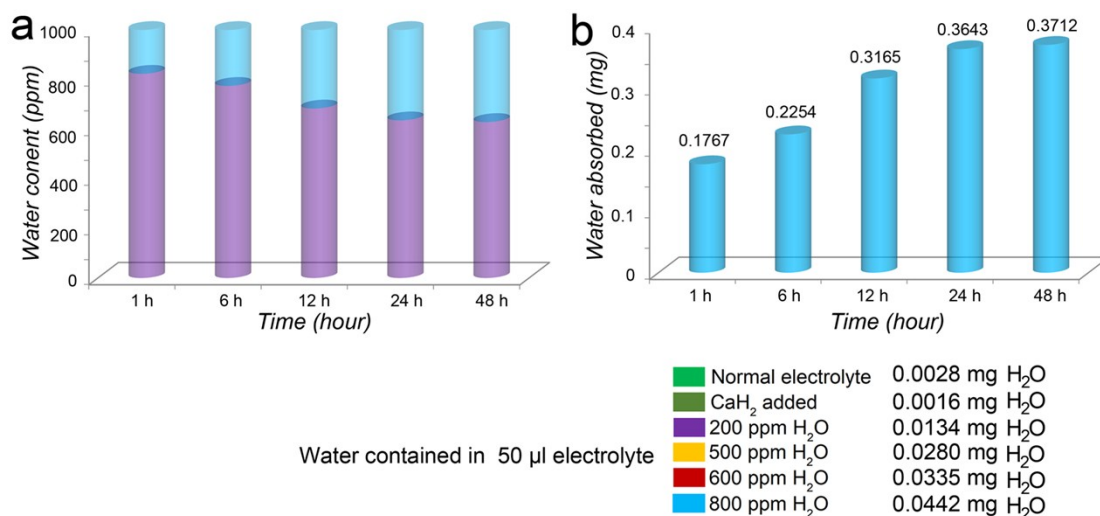
Figure S7. The maximum water adsorption capacity of the prepared MOF powder. (a) 50 mg MOF powder immersed into 1 mL 1000 ppm water contained electrolytes to probe the amount of the remained water. (b) The corresponding calculated water adsorption ability of 50 mg MOF powder and the accurate water contents in different electrolytes (50 µL for each cell) used in fabricating coin cells. As the MOF mass loading in MOF separator is 5 mg (16 mm in diameter), the MOF separator calculated can maximally adsorb 0.03712 mg water based on Fig. S7b. Clearly, MOF can effectively adsorb water contained in even 600 ppm water added electrolyte.
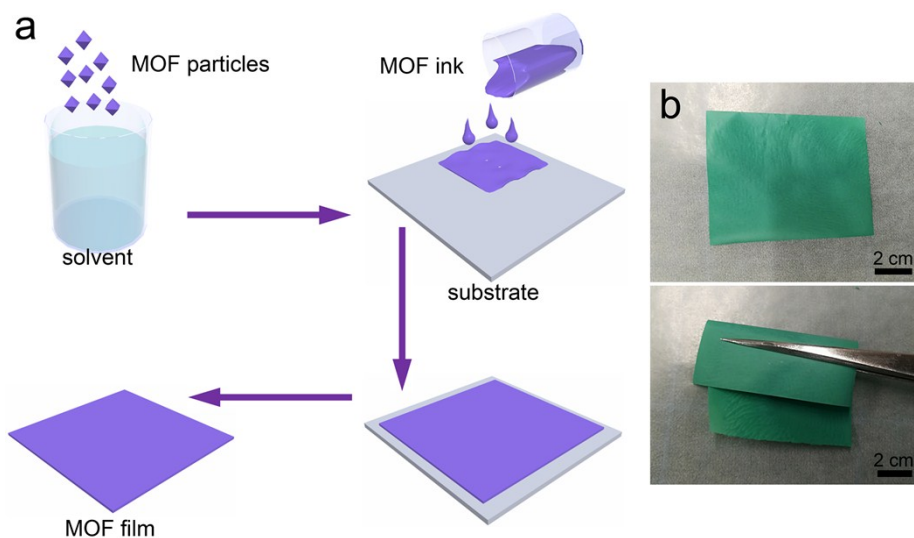
Figure S8. The preparation of the MOF separator. (a) Schematic illustration of the preparing process and (b) the corresponding digital photos of the flexible MOF separator. MOF powder was firstly dispersed in organic solvent (acetone) and then mixed with PVDF (in DMF) to form MOF slurry before coated on the surface of Al foil. After peeled off from the Al substrate, a MOF film with great flexibility was obtained.
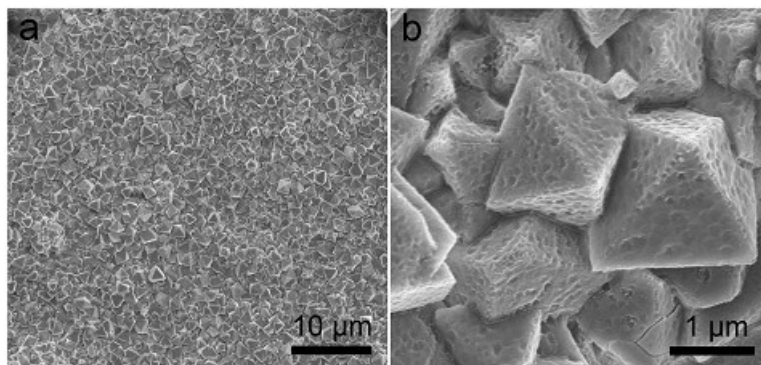
Figure S9. (a and b) SEM images of the prepared MOF separator. MOF particles tightly attached to each other and form a closely packed MOF separator. The obtained MOF separator maintains a thickness of nearly 30 μm (corresponding to 5 mg cm^{-2} CuBTC mass loading) with MOF particles tightly attached to each other.
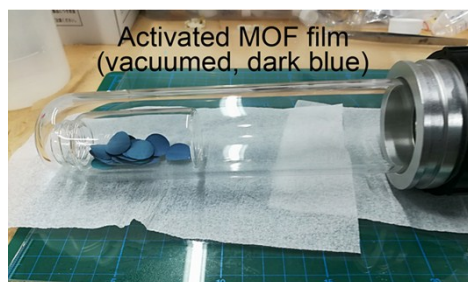
Figure S10. The activated MOF separators before transferred into the glove box. Before transferred into the glove box for cell fabricating, the prepared flexible MOF separators must subjected to another activated process to get rid of any possible moisture (The apparent color change from light green shown in Fig. S8b to dark blue suggesting the successful water removing of the activated MOF separators). The activated MOF separators were then transferred into the glove box in vacuum tube for cell fabrications.
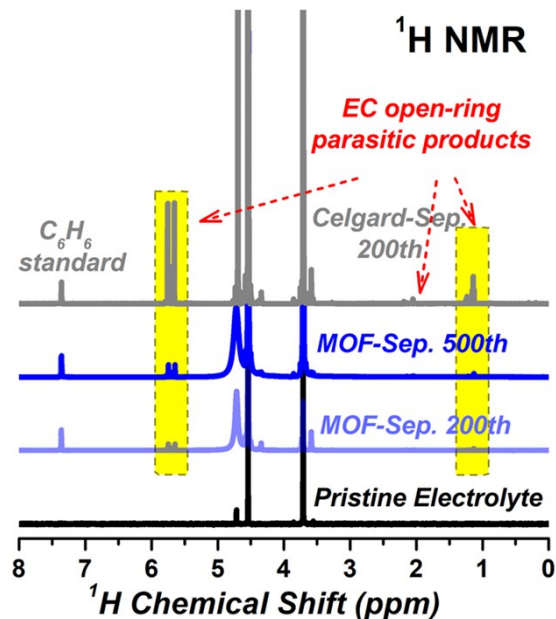
Figure S11. The MOF separator used as water scavenger enabled largely suppressed detrimental effects induced by water contained in electrolytes for Li//LiNi$_{0.5}$Mn$_{1.5}$O$_4$ (LNMO) batteries. ^{1}H analysis result of electrolytes harvested from cells cycled in commercial electrolyte using MOF (blue traces) and Celgard (grey traces) separators. ^{1}H NMR spectra of D$_2$O extracted components from cycled electrolytes. The spectra of the pristine electrolytes are shown on the bottom (black traces). By normalizing the peak of C$_6$H$_6$ inner standard, the degradation products are quantitatively estimated. The EC open-ring parasitic products can be clearly observed in LNMO cell assembled with Celgard separator, while that of the electrolyte extracted from MOF separator employed cell shown largely alleviated electrolyte decomposition parasitic products after 200 cycles. Even after 500 cycles, the electrolyte decomposition products from the MOF separator used cell are still much lower than that of the cell using Celgard separator.
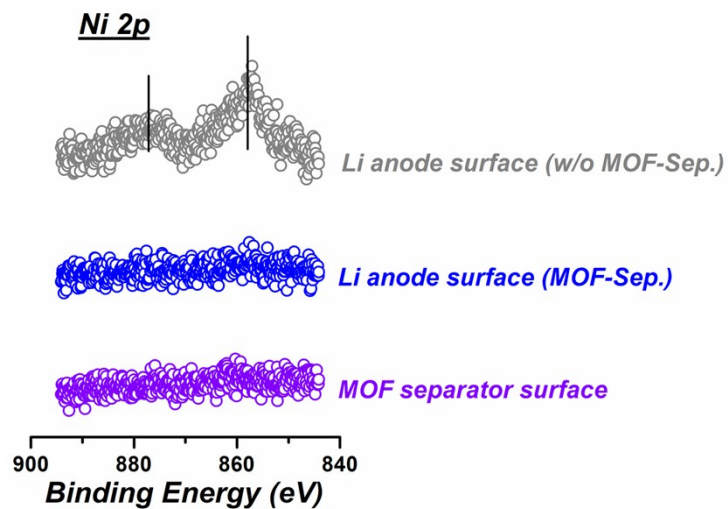
Figure S12. XPS spectra of the cycled Li anodes harvested from LNMO cells assembled with Celgard and MOF separators in Mn 2p region (after 400 cycles), indicating MOF separator can eliminate the shuttling/re-deposition of transition metal ion (Ni) on Li anode.
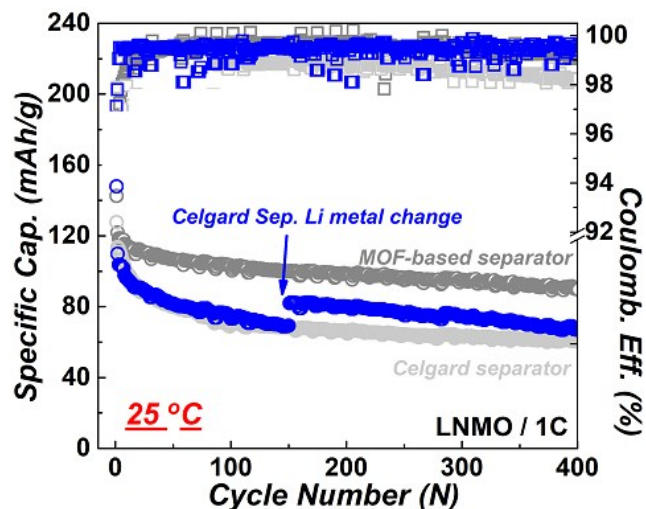
Figure S13. The capacity decay caused by the Li anode degradation related to water existed in cells. Cycling performance of the Li//LNMO cells (LNMO) using Celgard and MOF separators. The blue arrow indicates the point (at the end of 150th cycle) when the Li metal counter electrode of the Celgard separator used cell is replaced with a fresh one. The capacity gap between two Celgard separator used cells suggests the Li anode decay caused by detrimental effects of water. Note that, even slightly enhanced capacity was obtained for the Li anode replaced cell, the apparent capacity gap (about 20 mAh g^{-1}) between the MOF separator used LNMO cell and Celgard separator used LNMO cell with fresh Li change indicates the capacity loss caused by TM loss in Celgard based cell, which highlight the importance of extruding water by using MOF separator.
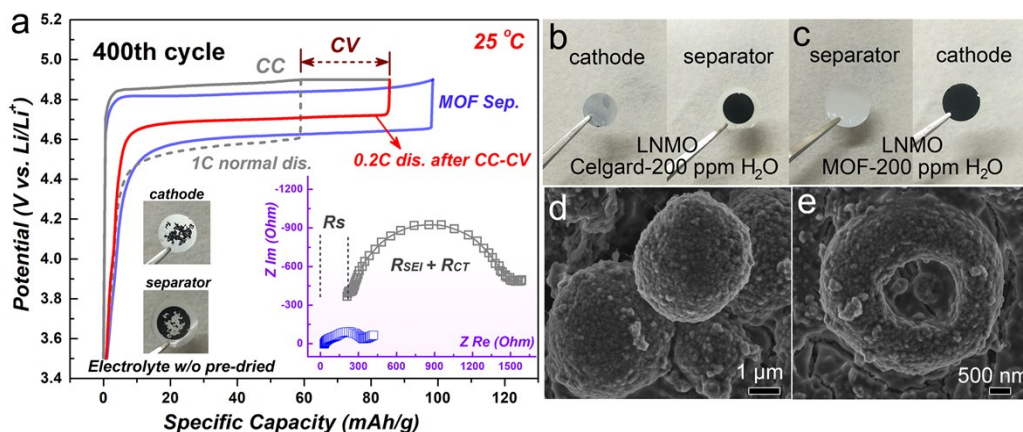
Figure S14. An additional electrochemical treatment on the cycled Li//LNMO cells (MOF separator based cell, the blue trace; Celgard separator based cell, the light grey and red traces). (a) The final target is to further analysis the influence of both resistance and metal-dissolution towards capacity loss. After 400 cycles (blue trace), the LNMO cathode was extracted and re-assembled into a new cell. After galvanostatic charging (CC mode) to the cut-off voltage (4.9 V vs. Li/Li$^+$), the cell was continuously keeping at 4.9 V (CV mode) until the current density drop to 5% (7.4 mA g^{-1}) of initial charging current rate (1C, 147 mA g^{-1}). Then the cell was discharged to 2.0 V. Corresponding Nyquist plot inset showing the impedance evolution of discharged Li//LNMO cells cycled using different separators. (b-d) Digital photos and SEM image of the cycled LNMO cathodes from the Celgard and MOF separators based cell (deliberately cycled in 200 ppm water added electrolyte). The structure remained LNMO particles also indicates the effectiveness of the MOF separator in protecting LNMO cathode against TM loss induced by water.
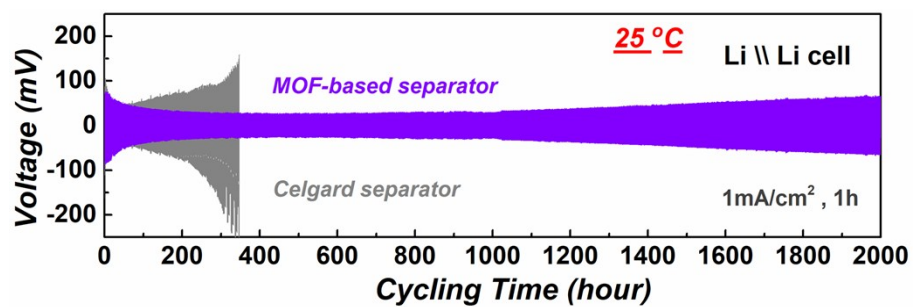
Figure S15. Li//Li symmetrical cell electrochemical performances of Celgard (light grey curve) and MOF-based separator (light purples curve) cycled in none pre-dried electrolyte (56.4 ppm water contained) at a current density of 1 mA cm^{-2}.
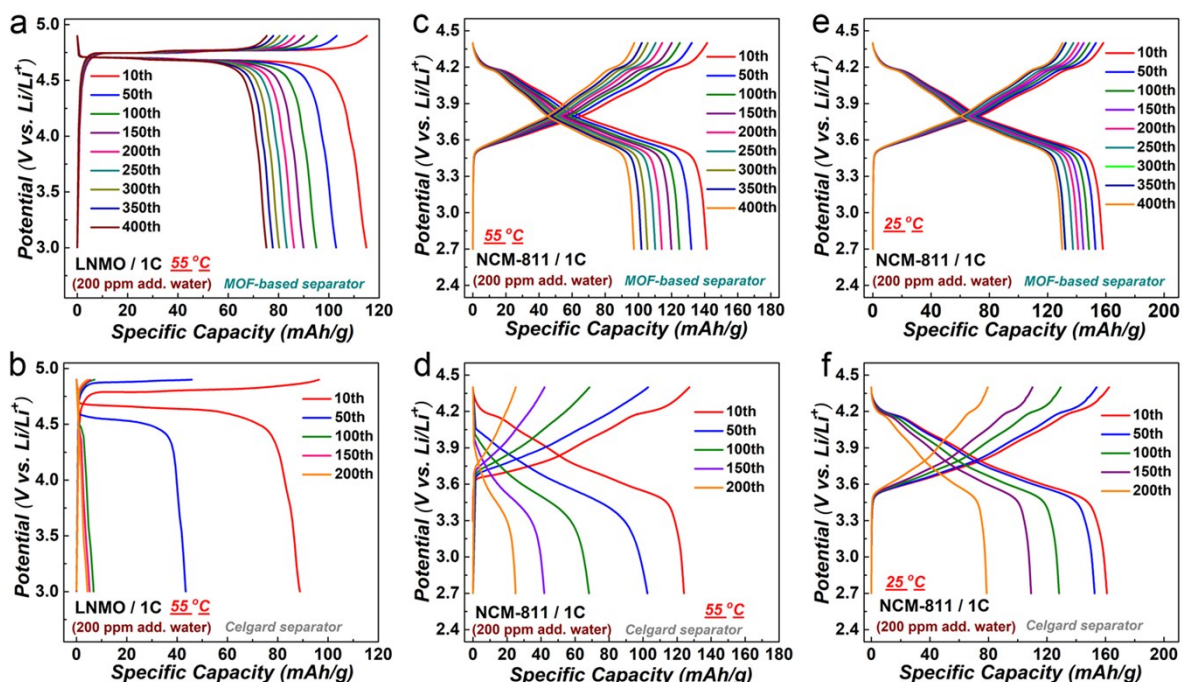
Figure S16. Charge/discharge curves of MOF and Celgard separators used lithium metal based rechargeable cells using 200 ppm water added electrolyte. (a and b) Charge/discharge curves of Li//LiNi$_{0.5}$Mn$_{1.5}$O$_4$ (LNMO) cells using (a) MOF and (b) Celgard based separator at 1 C current rate under evaluated temperature of 55 °C. (c and d) Charge/discharge curves of Li//LiNi$_{0.8}$Co$_{0.1}$Mn$_{0.1}$O$_2$ cells (NCM-811) using (c) MOF and (d) Celgard based separator at 1 C current rate under evaluated temperature of 55 °C. (e and f) Charge/discharge curves of Li//LiNi$_{0.8}$Co$_{0.1}$Mn$_{0.1}$O$_2$ cells (NCM-811) using (e) MOF and (f) Celgard based separator at 1 C current rate under room temperature of 25 °C. Compared with the Celgard based cells cycled under the same situations, MOF separator based cells delivered much better cycling stabilities and exhibited largely alleviated cell polarizations.
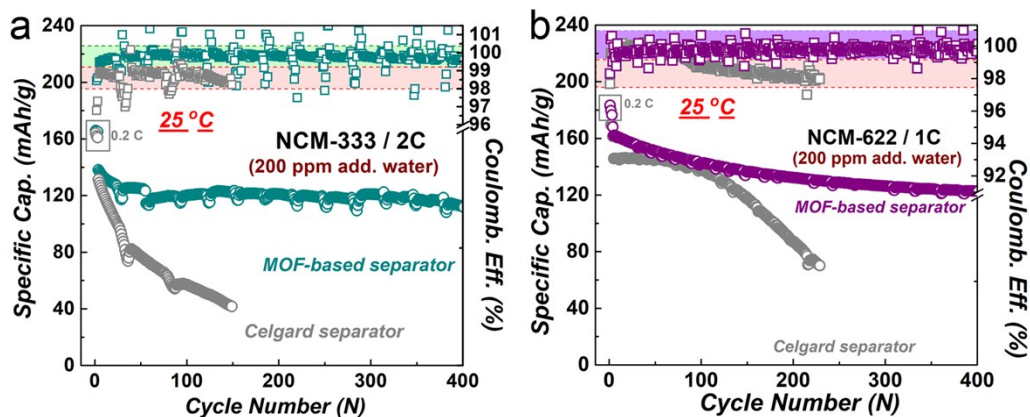
Figure S17. Electrochemical performances of MOF separators employed lithium metal rechargeable batteries (cycled in electrolyte with 200 ppm water added): Cycling performances of Celgard and MOF separator based cells in electrolyte containing 200 ppm water of (a) Li//LiNi$_{0.3}$Co$_{0.3}$Mn$_{0.3}$O$_2$ cells (NCM-333) and (b) Li//LiNi$_{0.6}$Co$_{0.2}$Mn$_{0.2}$O$_2$ (NCM-622) cells at 1 C current rate under room temperature of 25 °C.
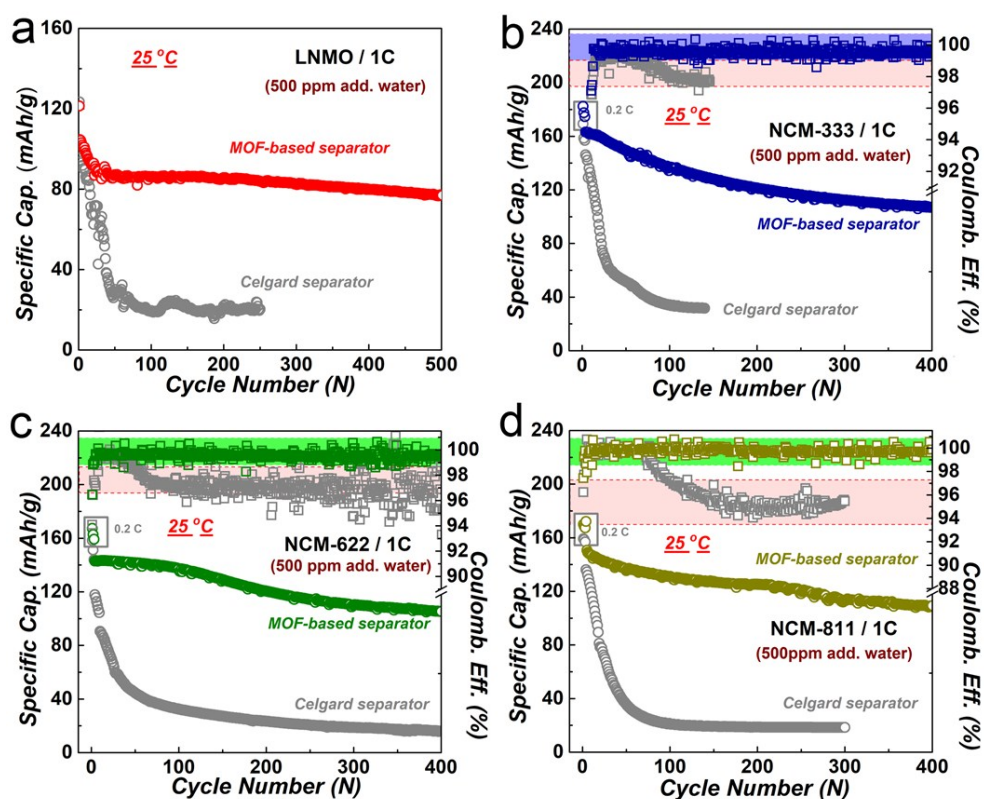
Figure S18. Electrochemical performances of MOF separator used lithium metal rechargeable batteries cycled in electrolytes containing 500 ppm water under room temperature of 25 °C: Cycling performances of (a) Li//LiNi$_{0.5}$Mn$_{1.5}$O$_4$ (LNMO), (b) Li//LiNi$_{0.3}$Co$_{0.3}$Mn$_{0.3}$O$_2$ (NCM-333), (c) Li//LiNi$_{0.6}$Co$_{0.2}$Mn$_{0.2}$O$_2$ (NCM-622) and (d) Li//LiNi$_{0.8}$Co$_{0.1}$Mn$_{0.1}$O$_2$ (NCM-811) cells with Celgard and MOF based separators at 1 C current rate. Typically, all those cells using Celgard separators cycled in 500 ppm added electrolytes experienced very quick capacity decay (capacity less 40 mAh g^{-1} were preserved within 100 cycles), while MOF separator based cells delivered way better cycling stabilities.
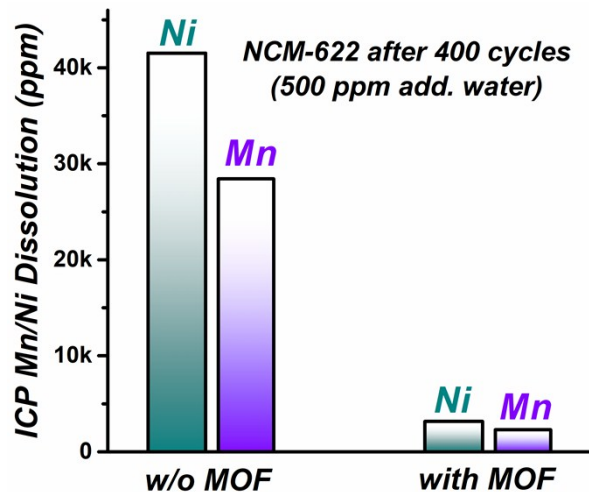
Figure S19. ICP analysis (Ni, Mn) results of the two Li//NCM-622 cells assembled with Celgard and MOF separators cycled in electrolytes containing 500 ppm water after 400 cycles. Note that the TM loss found in MOF separator used cell is much lower than that in Celgard separator used cell, suggesting largely suppressed TM loss after using MOF separator.
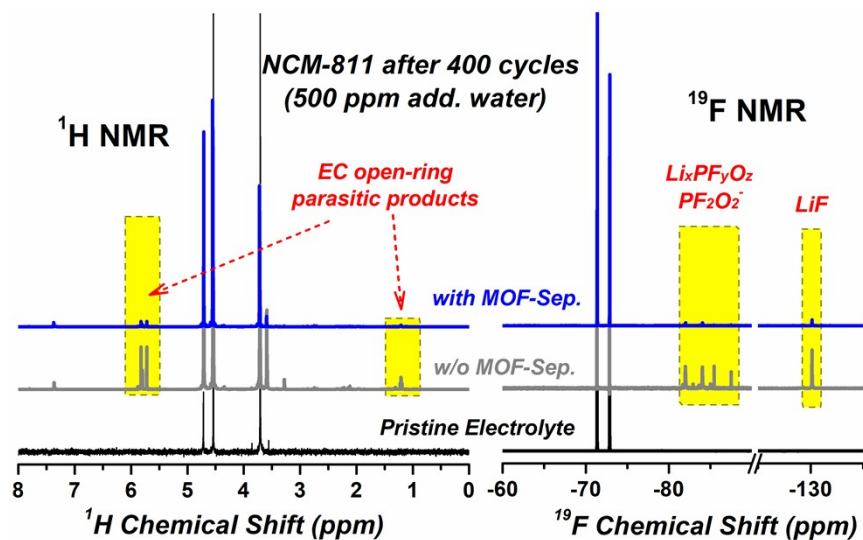
Figure S20. ^{1}H NMR and ^{19}F NMR analysis results of electrolytes from two Li//NCM-811 cells assembled with Celgard and MOF separators after cycled in electrolytes containing 500 ppm water for 400 cycles, showing greatly alleviated electrolyte decomposition parasitic products and accumulation of LiF after using MOF separator. ^{1}H and ^{19}F NMR spectra of D_2O extracted components from cycled electrolytes.
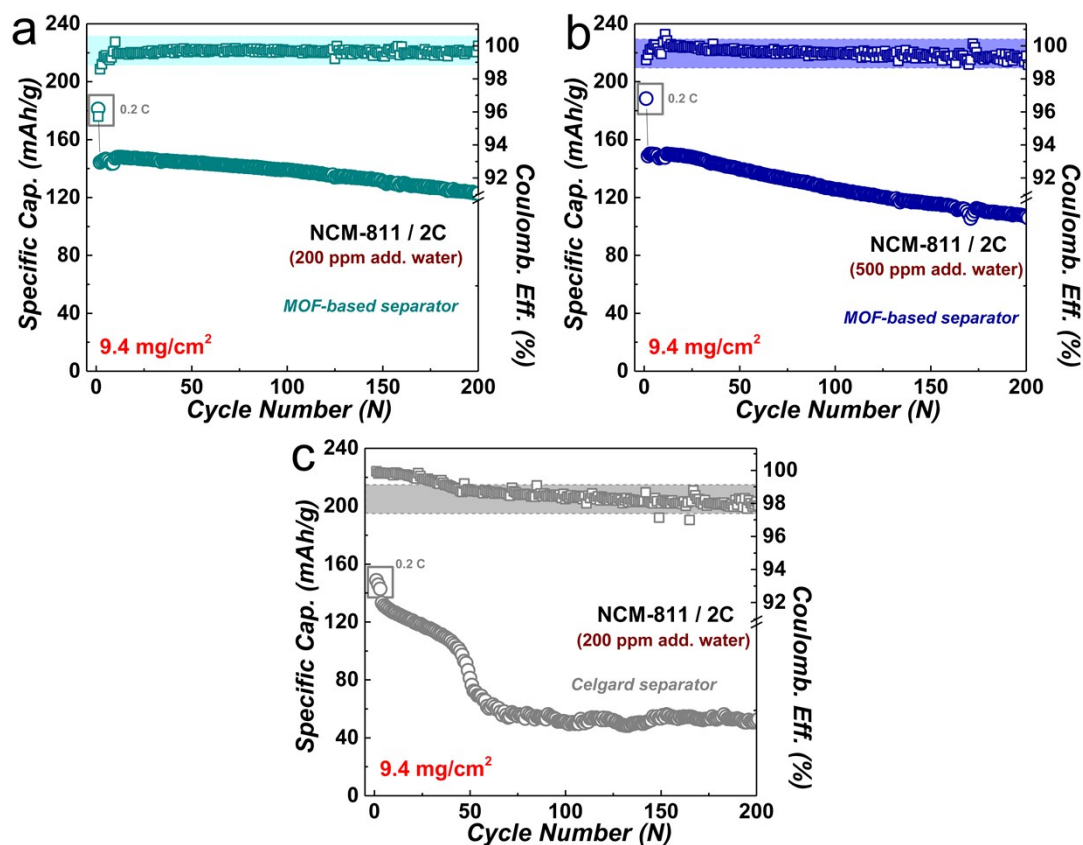
Figure S21. Cycling performances of the MOF based in-built water scavengers under high cathode mass loading Li//NCM-811 cell (9.4 mg/cm^2 NCM-811 for each cell) at 2 C within (a) 200 ppm and (b) 500 ppm water contained electrolytes. (c) Electrochemical performances of commercial Celgard separator used Li//NCM-811 batteries cycled in electrolytes containing 200 ppm water under high cathode mass loading Li//NCM-811 cell (9.4 mg/cm^2 NCM-811 for each cell) at 2 C.
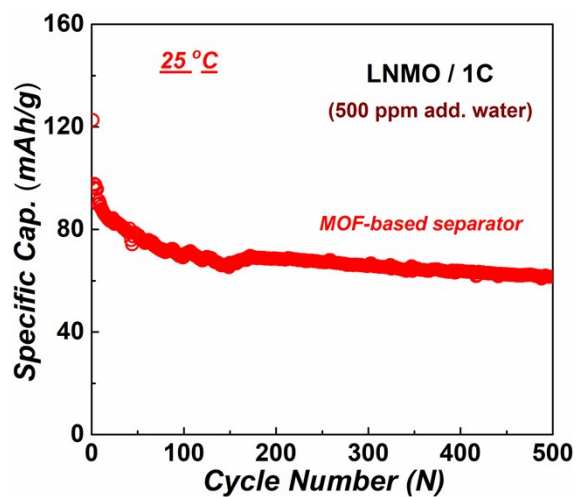
Figure S22. Cycling performances of the MOF separator based Li//LNMO cell at 1 C current rate under room temperature of 25 °C using 800 ppm water added electrolyte.
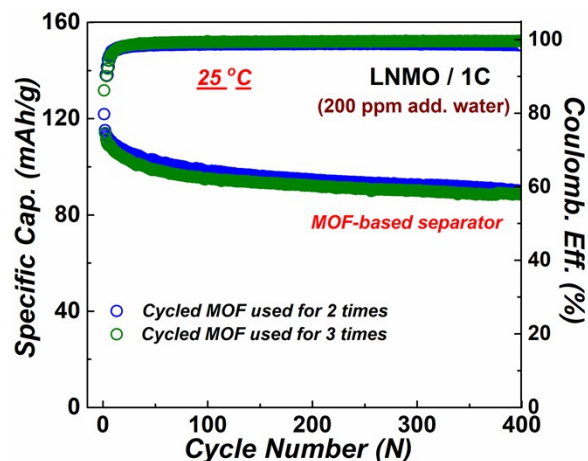
Figure S23. Cycling performance of the Li//LNMO cells using cycled MOF separators (blue curve for the second-hand MOF separator, green curve for the third-hand MOF separator) at 1 C current rate cycled in electrolyte containing 200 ppm water under room temperature of 25 °C. Obviously, even used for twice and third times, the MOF separator based two LNMO cells still delivered nearly the same cycling performances, which suggests the excellent recyclability of MOF separators. Note that, even used for three times, the capacity preserved are still at the same level of that of the Li//LNMO cell using fresh MOF separator, which again highlights the effectiveness of the MOF separator in scavenging water existed in lithium ion batteries.

References

1. Y. Qiao, S.-R. Li, Y. Yu and C.-H. Chen, *J. Mater. Chem. A*, 2013, **1**, 860-867.

2. Y. He, Z. Chang, S. Wu, Y. Qiao, S. Bai, K. Jiang, P. He and H. Zhou, *Adv. Energy Mater.*, 2018, **8**, 1802130.

3. M. S. Denny, M. K. Kalaj, C. Bentz and S. M. Cohen, *Chem. Sci.*, 2018, **9**, 8842-8849.

4. Y. Qiao, S. Wu, J. Yi, Y. Sun, S. Guo, S. Yang, P. He and H. Zhou, *Angew. Chem. Int. Ed.*, 2017, **56**, 4960-4964.

5. Y. Qiao, J. Yi, S. Wu, Y. Liu, S. Yang, P. He and H. Zhou, *Joule*, 2017, **1**, 359-370.

6. M. Xu, L. Zhou, Y. Dong, Y. Chen, A. Garsuch and B. L. Lucht, *J. Electrochem. Soc.*, 2013, **160**, A2005-A2013.